RSC Advances

ROYAL SOCIETY OF CHEMISTRY

www.rsc.org/advances

Cite this: DOI: 10.1039/c0xx00000x

www.rsc.org/xxxxxx

ARTICLE TYPE

Hierarchical porous nano-MFI zeolite-pillared montmorillonite clay synthesized by recrystallization for hydrocracking of residual oil

Zhiming Ren,[a] Baoshan Li,*[a] Liwen Yue,[b] Naijin Wu,[a] Kaixuan Lv,[a] Chunying Han,[a] Jianjun Liu[a]

Received (in XXX, XXX) Xth XXXXXXXXX 20XX, Accepted Xth XXXXXXXXX 20XX

DOI: 10.1039/b000000x

A MFI zeolite nanosheet-pillared montmorillonite clay (MPC) composite material has been synthesized under hydrothermal conditions by a recrystallization method. The hierarchical porous material possesses uniform micropores in the crystalline zeolite pillars and uniform mesopores between the zeolite pillars in the clay interlayer galleries. The MPC material exhibited higher activity and better selectivity in hydrocracking of residual oil than either MFI or montmorillonite clay pillared with silica (SPC) or the mixture of both.

Zeolites—microporous crystalline aluminosilicates—are widely used in petrochemistry and fine-chemical synthesis[1-3] since the strong acid sites within their uniform micropores enable size- and shape-selective catalysis. However, the microporous nature of zeolites imposes diffusion limitations in the case of bulky molecules.[4-8] Mesoporous aluminosilicate materials with various structures have been synthesized since the 1990s, following the synthesis of MCM-41 using surfactant micelles as templates.[9,10] However, such mesoporous materials are composed of amorphous frameworks and have insufficient acidity for most petrochemical reactions.[11,12] In recent years, a variety of methods—such as direct synthesis using different templating strategies, generation of mesopores in zeolite single crystals by post-synthesis treatment, zeolitization of mesoporous materials and recrystallization of zeolites—have been suggested as strategies for the synthesis of mesoporous materials having crystalline nanozeolitic micropore walls.[13] Of these methods, recrystallization of zeolites has attracted the most attention, because it is a simple and inexpensive way to create nanocrystalline microporous zeolites in a mesoporous material.[14–17] However the particle size and crystallinity of nano–microporous zeolites are difficult to control when using conventional mesoporous aluminosilicate materials, such as MCM-41, as a precursor.[18] Employing a mesoporous material that can restrict the unlimited growth of the microporous zeolite is required in order to solve this problem. Montmorillonite (MMT) is one such material, since it has good hydrothermal stability and a layered structure which should restrict the growth of microporous zeolites in the third direction.[19-21]

In the last few years, there have been many reports of modulation of the pore structure within the interlayer galleries of MMT.[21-24] For example, MMT pillared with silica (SPC) has a large number of mesopores, leading to many catalytic applications.[23,25] However there have been no reports of the introduction of a crystal microporous zeolite into the interlayer galleries of MMT.

In this work, we use MFI zeolite as an example of a microporous zeolite and show how it can be incorporated in the interlayer galleries of MMT by a zeolite recrystallization method, using SPC as the precursor and tetrabutylammonium bromide (TBAB) as a template, to give a nano-MFI pillared MMT clay (MPC). The synthesis procedure is illustrated in Scheme 1 in the ESI. According to the recrystallization time of 3d, 4d and 5d, the samples were named MPC-3, MPC-4 and MPC-5, respectively.

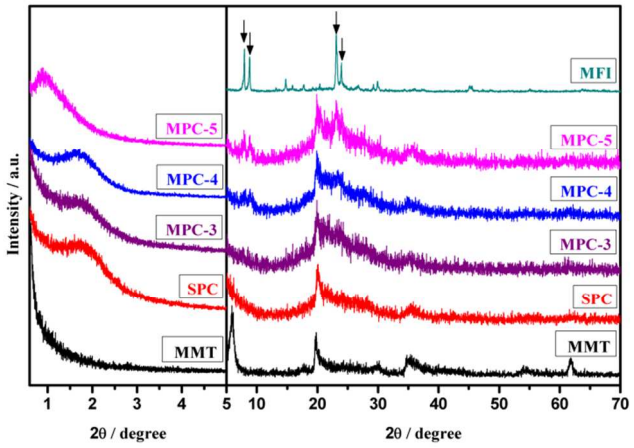

Fig. 1 XRD patterns of MFI, MPCs, SPC and MMT.

Fig. 1 shows the XRD patterns of ZSM-5 zeolite, MPCs, SPC and MMT. The XRD pattern of SPC shows three sharp peaks at 20°, 29°, and 36° and one weak broad feature at 62° 2θ. These peaks can be indexed to the (110), (020), (004), (130), (200), (330) and (060) reflections of MMT, [26] showing that the crystalline structure of the clay sheets has not been destroyed by incorporation of silica. In addition, an intense peak appears in the low-angle diffraction pattern of SPC at around 1.7° 2θ, corresponding to an interlayer distance of 5.2 nm, which has been increased 3.6 nm comparing with the interlayer distance of MMT (1.6 nm). After recrystallization for 4 d, the peaks of SPC were retained, and two weak peaks appeared in the wide-angle diffraction pattern at 7.9°, 8.9° with a wide diffraction peak appeared in 23.1° 2θ, which indicates that the crystal particles are at the nano-scale[23]. These new peaks can be attributed to the

formation of MFI-type zeolite. Furthermore, the intensity of the diffraction of MFI increased as the recrystallization time was prolonged to 5d. And a new peak also appeared in the low-angle diffraction pattern at 0.88°, which indicates that the interlayer distance has increased by 4.6 nm to 9.8 nm after recrystallization of SPC. This is consistent with the generation of MFI zeolite between the lamellae of MMT as a result of the recrystallization.

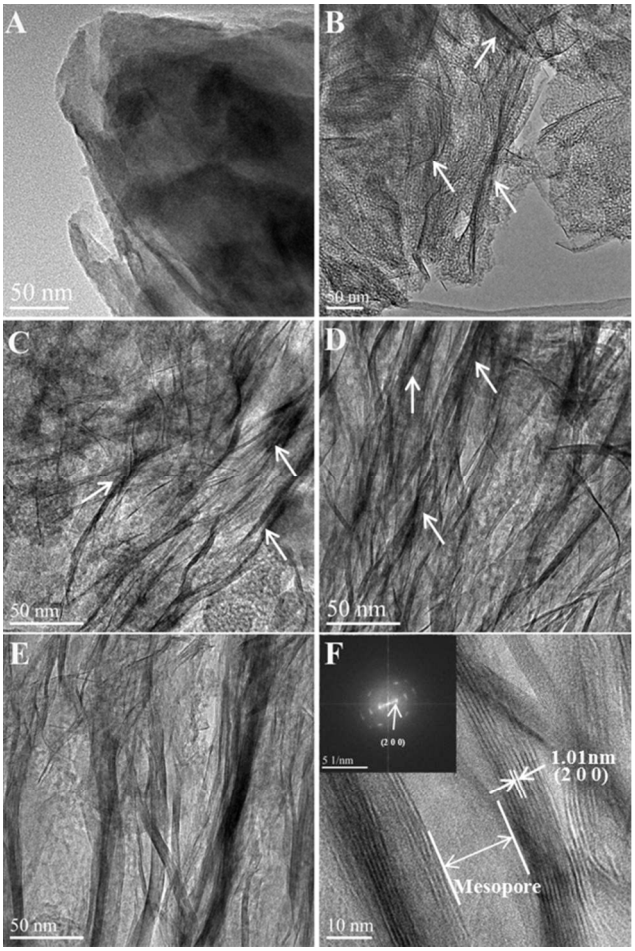

Fig. 2 HRTEM images of (A) MMT, (B) SPC, (C) MPC-3, (D) MPC-4, (E) MPC-5 and (F) MPC-5 at high magnifications.

Fig. 2 shows HRTEM images of MMT (Fig. 2A), SPC (Fig. 2B) and MPCs (Fig. 2C to Fig. 2F). As shown in Fig. 2A, no mesoporous or microporous framework was observed in MMT, consistent with previous reports[24, 27]. After MMT was pillared by silica to give SPC, some black stripes—which are consistent with the formation of silica pillars—can be observed in the interlayer galleries clearly (Fig. 2B marked by arrows). Although they generate a mesoporous structure between the lamellae of MMT, the pillars are distributed in a sparse and irregular manner. However, when the SPC was recrystallized for 3d (Fig. 2C), the black stripes become concentrate. Furthermore, the black stripes become wider and clearer (Fig. 2D marked by arrows) as the recrystallization time was prolonged to 4d. Moreover, when MPC-5 was synthesized by recrystallization of SPC for 5d, more regularly distributed nano-MFI zeolite particles about 10 nm in size can be observed between the lamellae of MMT (Fig. 2E). At higher magnification, fine lines indicative of a uniform microporous framework can be clearly seen in the interlayer galleries of MPC-5 (Fig. 2F marked). The lattice spacing of these fringes (1.01 nm) is the same as that of the pure MFI (see Fig. 1S in the ESI), and consistent with the (200) reflection of MFI observed at 2θ 8.8° in its XRD pattern (Fig. 1).

The even distribution of these nano-zeolite crystals shows that the confinement effect of the MMT layers provides a way of overcoming the usual problem of aggregation of nano-zeolite particles. The resulting pillared material possesses a structural hierarchy on two different length scales—mesopores due to the slits between the clay layers pillared by the zeolite, and micropores due to the MFI nano-zeolite framework (see Fig. 2F).

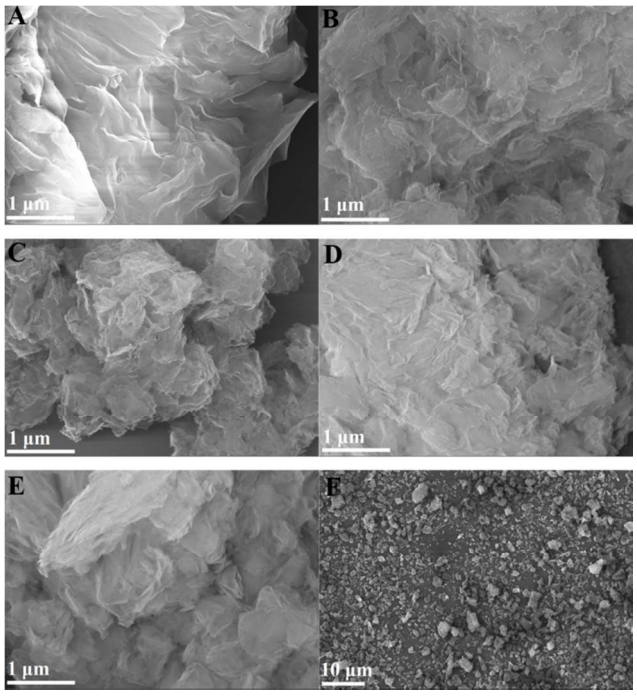

Fig. 3 SEM images of (A) MMT, (B) SPC, (C) MPC-3, (D) MPC-4, (E) MPC-5 and (F) MPC-5 at low magnifications.

In order to investigate the transformation of the morphology of MPC as the recrystallization time was increased, the samples were studied by SEM (Fig. 3). It can be observed that the overall morphology of the MMT was retained after formation of MPCs. Furthermore, although the roughness of the surfaces increased, no MFI crystals can be observed on the exterior of the MPCs. It can also be observed that as the recrystallization time was prolonged, the layered structure of MMT was becoming more and more fluffy. Furthermore, when pure MMT was recrystallized under the same conditions as those for used for SPC, no diffraction peaks of MFI were observed (Fig. 2S in the ESI), confirming that MFI is unable to form on the external surfaces of MMT.

The process of zeolite recrystallization can be explained by a 'solution-mediated' mechanism.[28] According to this mechanism, a gel-type or solid-like silica source becomes partially dissolved during the initial stage of crystallization, so that there is equilibrium between undissolved and dissolved species. The dissolved species re-assembles into a crystalline zeolite with the aid of a template. If the mobility of the dissolved species is very high, it can migrate to a remote growth site in the developing crystals and consequently, the morphology of the zeolite crystal can be very different from the initial gel morphology.

Table 1 Catalytic performance for hydrocracking of residual oil.

Samples	Conversion (%)	Product yield (%)				
		Gas	Gasoline	Kerosene	Coke	Others
6%NiO/MPC-3	70.1	1.5	48.5	43.1	4.6	2.3
6%NiO/MPC-4	73.8	1.7	68.1	22.3	5.2	2.7
6%NiO/MPC-5	81.2	2.6	75.8	12.7	6.8	2.1
6%NiO/SPC	67.3	1.3	46.7	43.7	3.0	5.3
6%NiO/ZSM-5	32.7	8.2	66.9	7.1	14.1	3.7
6%NiO/(SPC&ZSM-5)	58.2	6.5	56.6	23.0	11.0	2.9

a

On the other hand, if the mobility is very low, or the dissolved silicate species is immediately captured by a template to form a zeolite crystal, the morphology of the initial gel is maintained in the final product.[29] In our synthesis process, we employed a tetrabutylammonium ion (TBA^+) template which captures the amorphous silica pillars which dissolve in the solution, and forms the MFI zeolite crystals between the clay layers. The confinement effect of the MMT layers limits the mobility of the dissolved silica between the layers and reduces the rate of growth of MFI zeolite, which favours the formation of nano-MFI zeolite in the initial stages of crystallization. However prolonged crystallization results in a change in morphology of the zeolite, which is consistent with a previous study.[30]

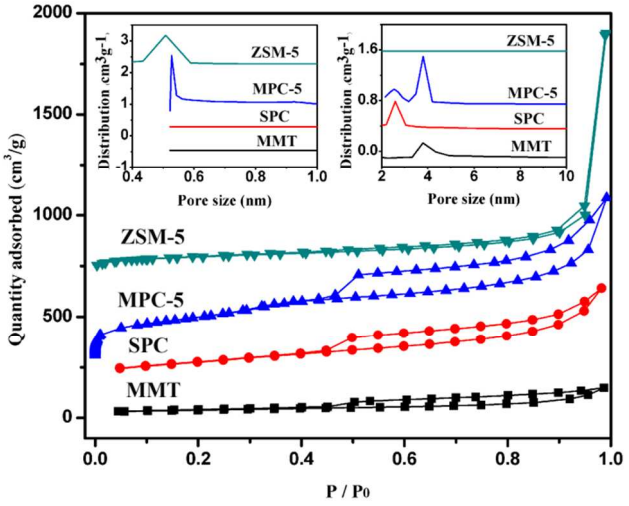

Fig. 4 N_2 adsorption–desorption isotherms and pore size distribution of MMT, SPC, MPC-5 and ZSM-5. (The isotherms for the samples of MMT, SPC, MPC-5 and ZSM-5 are offset vertically by 74, 164, 305, and 694 cm^3 g^{-1}, respectively.)

The N_2 adsorption–desorption isotherms of MMT, SPC, MPC-5 and ZSM-5 are shown in Fig. 4. The ZSM-5 sample showed a type I adsorption isotherm, in which the adsorption amount was saturated in an extremely low relative pressure region ($P/P_0 < 0.05$) as a result of monolayer adsorption of N_2 inside the micropores. SPC shows a type IV isotherm with adsorption hysteresis (H3), which is characteristic of a slit-type mesoporous structure. The MPC-5 can also be characterized as the type IV, whose feature correspond to the type B in the Boer's five types representing the presence of open slit-shaped pores formed in gallery regions. There are two peaks in the mesopore pore size distribution plot at diameters of 2.54 nm and 3.80 nm (Fig. 4 inset). The former can be attributed to the mesopores formed during the preparation of the SPC precursor (see the mesopore pore size distribution in Fig. 4). The latter larger pores are associated with the expansion of the interlayer gallery height resulting from the formation of nano-zeolites between the clay layers during the recrystallization process. The micropore diameter distribution in MPC-5 was determined by analysing its N_2 adsorption isotherm and subsequently converting it into a micropore size distribution according to nonlocal density functional theory. The result indicates that the micropore diameter (0.53 nm) of MPC-5 is exactly the same as that of ZSM-5. The Brunauer–Emmett–Teller (BET) surface area and total pore volume of MPC-5 after calcination are 734 m^2 g^{-1} and 1.21 cm^3 g^{-1}, respectively. Moreover, the micropore volume of MPC-5 was 0.17 m^3 g^{-1} (calculated by Horvath-Kawazoe method), indicating that 14.0% of mesopore has been converted into micropore during the recrystallization process. More details of the pore structure parameters of the samples can be seen in Table 1S in ESI.

The acidities of MPC-5, SPC and ZSM-5(Si/Al=12) were analysed by NH_3-TPD, and the results show that the acidities of MPC-5 and SPC were a little higher than ZSM-5(Si/Al=12), owing to the strong acidity of MMT layer (Fig. 3S and Table 3S in ESI). Moreover, the catalytic performance of MPC-5, SPC and ZSM-5(Si/Al=12) in the isomerization of *m*-xylene to *p*-xylene shows that the micropores in the pillars are intimately associated with the surface of the host clay layers (Table. 4S in ESI). Thus, the MPCs were proved to be nano-zeolite pillared montmorillonite with hierarchical porous structure, but not a mechanical mixture of SPC and MFI.

The catalytic activity of the MPCs and the compared samples after loading 6 wt. % nickel oxide were evaluated in the hydrocracking of residual oil. The samples were denoted as 6%NiO/MPC-3, 6%NiO/MPC-4, 6%NiO/MPC-5, 6%NiO/SPC, 6%NiO/ZSM-5 and 6%NiO/ (SPC&ZSM-5), and the catalytic results are shown in Table 1. The reaction product was separated into gaseous and liquid products, and the different distillation range oil was obtained by distillation of the liquid products. According to the boiling range of petroleum products, the composition of petroleum distillates was defined to gasoline fraction (70-120 ℃), which is the main components of high-value, middle distillates, and kerosene fraction (120-150 ℃).

6%NiO/SPC showed 67.3% conversion of residual oil and 46.7% selectivity for gasoline (Table 1, no. 4). 6%NiO/MPC-4 showed obviously increased conversion (73.8%) and gasoline selectivity (68.1%) (Table 1, no. 2). The improvement is presumed to be the contribution of the micropores of MFI zeolite in the interlamellar of MMT, having uniform and regular pore sizes and high acidities. Further, 6%NiO/MPC-5 exhibits the best

conversion (81.2%) of residual oil and highest selectivity (75.8%) of gasoline. This is good indication, more and more MFI zeolite with microporous structure has been generated in the MPC-5 material after hydrothermal treatment, constituting a good hierarchical micro–mesoporous structure. Compared with the conversional ZSM-5 zeolite, the mesopores between the nano-zeolite pillars shorten the diffusion paths of molecules and help them to reach the zeolite acid sites more easily. Besides, the middle distillates of gasoline can diffuse out of the micropores immediately, inhibiting deep cracking and suppresses the formation of gaseous hydrocarbons. The catalytic activity of conversional ZSM-5 zeolite was also tested. The conversion was only 32.7%, much lower than the other catalyst, which can be contributed to the fact that the macromolecule in the residual oil has some difficulty in diffusing into the micropores of zeolite. And because traditional ZSM-5 catalyst has the deep cracking ability in hydrocracking reactions, the selectivity of gas was pretty high, up to 8.2%. The mechanical mixture of SPC and ZSM-5 was also employed in the hydrocracking, exhibiting a lower conversion of residual oil (58.2%) and lower selectivity for gasoline (56.6%) compare with MPC-5. This result also indicates that the MPCs are not a mechanical mixture of SPC and MFI, but a hierarchical porous material with nano-zeolite between the MMT layers.

Thus, nano-zeolite pillared montmorillonite hierarchical porous material not only has high activity for hydrocracking of macromolecule, but also exhibits good selectivity for gasoline. In a more detailed comparison, 6%NiO/MPC-5 always showed a higher conversion of residual oil and a higher selectivity for gasoline than 6%NiO/SPC during 25 h time-on-stream (Fig. 4S in ESI).

In summary, we have discovered a new inexpensive process for producing microporous nano-zeolites and preventing their aggregation. A nano-MFI zeolite sieve was introduced into the interlamellar galleries of MMT to give nano-MFI pillared montmorillonite clay (MPC) with a hierarchical micro–mesoporous structure. XRD SEM and TEM measurements show that the layered structure of MMT was not destroyed, and the nano-MFI zeolite was distributed evenly between the layers of MMT. A bimodal pore system was obtained with a narrow size distribution of micropores (centered at 0.53 nm) and mesopores (peaking at 2.54 nm and 3.80 nm). The MPCs exhibited higher activity and better selectivity in the catalytic hydrocracking of residual oil than either ZSM-5 or SPC or the mixture of both. This can be attributed to the even distribution of the nano-zeolite materials, combined with interconnected micropores and mesopores which help to overcome the diffusional limitations associated with conventional materials. We expect that our synthesis approach can be employed in the synthesis of other microporous zeolites leading to improved performances in a range of important catalytic applications.

Acknowledgement

We acknowledge the financial support from the National Natural Science Foundation of China (21271017) and the Fundamental Research Funds for the Central Universities (No.YS1406).

Notes and references

[a] *State Key Laboratory of Chemical Resource Engineering, Beijing University of Chemical Technology, No. 15 Beisanhuan East Road, Beijing 100029, P. R. China. Fax: (+) 86-010-64445611; Tel: (+) 86-010-64445611; E-mail: bsli@mail.buct.edu.cn*

[b] *Zhengzhou University of Light Industry, No. 5 Dongfeng Road, Zhengzhou, Henan Province 450002,P. R. China.*

† Electronic Supplementary Information (ESI) available: [details of the synthesis procedure and additional characterization data]. See DOI: 10.1039/b000000x/

1 C. S. Cundy, P. A. Cox, *Chem. Rev.*, 2003, ***103***, 663-701.
2 A. Corma, *Chem. Rev.*, 1997, ***97***, 2373-2419.
3 A. Corma, *J. Catal.*, 2003, ***216***, 298-312.
4 M. Choi, H. S. Cho, R. Srivastava, C. Venkatesan, D.-H. Choi, R. Ryoo, *Nat. Mater.*, 2006, ***5***, 718-723.
5 R. Srivastava, M. Choi, R. Ryoo, *Chem. Commun*., 2006, ***43***, 4489-4491.
6 M. Choi, K. Na, J. Kim, Y. Sakamoto, O. Terasaki, R. Ryoo, *Nature,* 2009, ***461***, 246-249.
7 J. Kim, M. Choi, R. Ryoo, *J. Catal.*, 2010, ***269***, 219-228.
8 J. Kim, W. Park, R. Ryoo, *ACS Catal.*, 2011, ***1***, 337-341.
9 C. T. Kresge, M. E. Leonowicz, W. J. Roth, J. C. Vartuli, J. S. Beck, *Nature,* 1992, ***359***, 710-712.
10 J. S. Beck, J. C. Vartuli, W. J. Roth, M. E. Leonowicz, C. T. Kresge, K. D. Schmitt, C. T. W. Chu, D. H. Olson, E. W. Sheppard, S. B. McCullen, J. B. Higgins, J. L. Schlenker, *J. Am. Chem. Soc.*, 1992, ***114***, 10834-10843.
11 K. Cassiers, T. Linssen, M. Mathieu, M. Benjelloun, K. Schrijnemakers, P. Van Der Voort, E. F. Vansant, *Chem. Mater.*, 2002, ***14***, 2317-2324.
12 D. Zhao, C. Xie, Y. Zhou, S. Xia, L. Huang, Q. Li, *Catal. Today*, 2001, ***68***, 11-20.
13 I. I. Ivanova, E. E. Knyazeva, *Chem. Soc. Rev.*, 2013, ***42***, 3671-3688.
14 Yu. P. Khitev, Yu. G. Kolyagin, I. I. Ivanova, O. A. Ponomareva,F. Thibault-Starzyk, J.-P. Gilson, C. Fernandez, F. Fajula, *Micropor. Mesopor. Mater.*, 2011, ***146***, 201-207.
15 S. Wang, T. Dou, Y. Li, Y. Zhang, X. Li, Z. Yan, *Catal. Commun.*, 2005, ***6***, 87-91.
16 H. Xu, J. Guan, S. Wu, Q. Kan, *J. Colloid Interface Sci.*, 2009, ***329***, 346-350.
17 S. Inagaki, M. Ogura, T. Inami, Y. Sasaki, E. Kikuchi, M. *Matsukata, Micropor. Mesopor. Mater.*, 2004, ***74***, 163-170.
18 X. Chen, S. Kawi, *Chem. Commun.*, 2001, ***15***, 1354-1355.
19 A. Ontam, N. Khaorapapong, M. Ogawa, *J. Mater. Chem.*, 2012, ***22***, 20001-20007.
20 J. Choy, J. Yoon, H. Jung, J. Park, *J. Mater. Chem.*, 2003, ***13***, 557-562.
21 H. Mao, X. Gao, J. Yang, B. Li, *Appl. Surf. Sci.*, 2011, ***257***, 4655-4662.
22 H. Mao, B. Li, X., Z. Liu, W. Ma, *Appl. Surf. Sci.*, 2009, ***255***, 4787-4791.
23 H. Zhang, D. Pan, and X. Duan, J. Phys. Chem. C, 2009, ***113***, 12140-12148.
24 H. Mao, B. Li, L. Yue, L. Wang , J. Yang, X. Gao, *Appl. Clay Science*. 2011, ***53***, 676-683.
25 H. Mao, K. Zhu, B. Li, C. Yao, Y. Kong, *Appl. Surf. Sci.*, 2014, ***292***, 1009-1019.
26 K. R. Kloetstra, H. V. Bekkum, J. C. Jansen, *Chem. Commun.*, 1997, ***23***, 2281-2282.
27 H. Mao, B. Li, X. Li, L. Yue, J. Xu, B. Ding, X. Gao, Z. Zhou, *Micropor. Mesopor. Mater.*, 2010, ***130***, 314-321.
28 C. S. Cundy, P. A. Cox, *Micropor. Mesopor. Mater.*, 2005, ***82***, 1-78.
29 M. Choi, K. Na and R. Ryoo, *Chem. Commun.*, 2009, ***20***, 2845-2847.
30 M. W. Anderson, S. M. Holmes, S. M. Holmes, N. Hanif, C. S. Cundy, *Angew. Chem., Int. Ed.*, 2000, ***39***, 2707-2710.
31 E. Dumitriu, V. Hulea, *J. Catal*. 2003, ***218***, 249-257.
32 J. Fei, Z. Hou, B. Zhu, H. Lou, X. Zheng, *Applied Catalysis A: General*, 2006, ***304***, 49-54.
33 F. J. Llopis, G. Sastre, A. Corma, *J. Catal.* 2006, ***242***, 195-206.

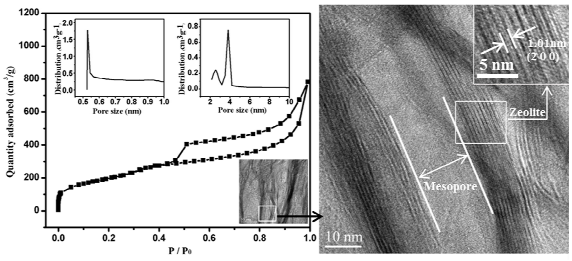

A MFI zeolite nanosheet-pillared montmorillonite clay (MPC) with uniform hierarchical structure was synthesized by a recrystallization method.